ACS APPLIED MATERIALS & INTERFACES

Research Article

www.acsami.org

Effect of Surface Topography and Bioactive Properties on Early Adhesion and Growth Behavior of Mouse Preosteoblast MC3T3-E1 Cells

Na Li,[†] Gang Chen,[†] Jue Liu,[†,△] Yang Xia,[†] Hanbang Chen,[†] Hui Tang,[†] Feimin Zhang,*[,†] and Ning Gu[‡]

[†]Jiangsu Key Laboratory of Oral Diseases, Nanjing Medical University, Nanjing 210029, China

[‡]Suzhou Institute & Collaborative Innovation Center of Suzhou Nano Science and Technology, Southeast University, Suzhou 215000, China

[△]The First People's Hospital of Changzhou, Changzhou 213000, China

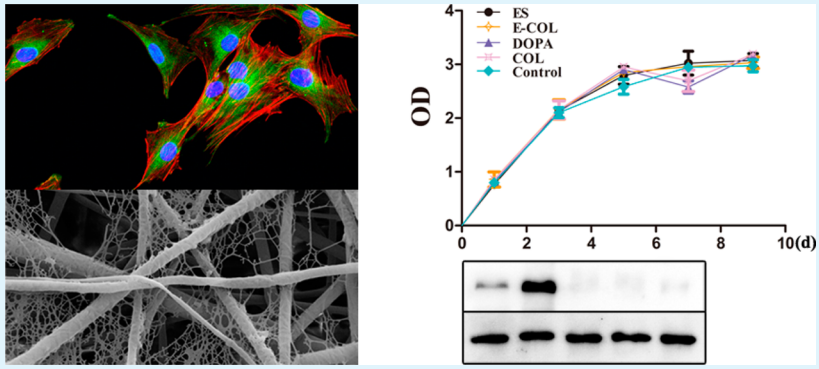

ABSTRACT: The effects of bioactive properties and surface topography of biomaterials on the adhesion and spreading properties of mouse preosteoblast MC3T3-E1 cells was investigated by preparation of different surfaces. Poly lactic-*co*-glycolic acid (PLGA) electrospun fibers (ES) were produced as a porous rough surface. In our study, coverslips were used as a substrate for the immobilization of 3,4-dihydroxyphenylalanine (DOPA) and collagen type I (COL I) in the preparation of bioactive surfaces. In addition, COL I was immobilized onto porous electrospun fibers surfaces (E-COL) to investigate the combined effects of bioactive molecules and topography. Untreated coverslips were used as controls. Early adhesion and growth behavior of MC3T3-E1 cells cultured on the different surfaces were studied at 6, 12, and 24 h. Evaluation of cell adhesion and morphological changes showed that the all the surfaces were favorable for promoting the adhesion and spreading of cells. CCK-8 assays and flow cytometry revealed that both topography and bioactive properties were favorable for cell growth. Analysis of β1, α1, α2, α5, α10 and α11 integrin expression levels by immunofluorescence, real-time RT-PCR, and Western blot and indicated that surface topography plays an important role in the early stage of cell adhesion. However, the influence of topography and bioactive properties of surfaces on integrins is variable. Compared with any of the topographic or bioactive properties in isolation, the combined effect of both types of properties provided an advantage for the growth and spreading of MC3T3-E1 cells. This study provides a new insight into the functions and effects of topographic and bioactive modifications of surfaces at the interface between cells and biomaterials for tissue engineering.

KEYWORDS: *integrin, adhesion, surface topography, bioactive properties*

INTRODUCTION

Because a bone defect does not heal in the same way as a normal wound, grafts of bone and its substitutes are now used as an effective solution to this problem. Currently, autografts, allografts, as well as grafts of alloplastics and synthetic bone are the most widely used strategies for grafting in bone tissue engineering.[1] Although autologous bone transplantation is the gold standard and allografting is an attractive alternative to autografts in bone repair, these procedures carries the risk of inducing a secondary trauma and immunological rejection. Therefore, an ideal bone substitute is required to circumvent the current difficulties.

Successful bone tissue regeneration requires at least three key factors: (I) the cells, (II) the scaffold that provides a structural support to the cells, and (III) cell−matrix (scaffold) interactions that direct bone tissue growth.[2] Three-dimensional (3D) scaffolds are also a key factor in bone tissue engineering. Tissue engineering now faces a major challenge in providing optimal interactions at the interface between scaffolds and cells. To mimic the structure of the cell-extracellular matrix (ECM),

Received: July 21, 2014
Accepted: September 11, 2014
Published: September 11, 2014

the topography and active chemical groups at the scaffold interface must provide support to the matrix-infiltrating cells. However, how differences in characteristics such as topography and biochemical properties (e.g., roughness, smoothness, solubility, and chemistry) at the interface correlate to differences in osteoconductivity and osteoinductivity remains to be elucidated. To date, reports have described various methods of surface modification for better cellular attachment, such as plasma treatment,[3] physical adsorption,[4] and chemical immobilization of ECM molecules and cell recognition peptides.[5]

In recent years, electrospinning has become a new and inexpensive nanofiber approach that has attracted significant public attention.[6] More than 100 different types of polymers have been produced as films by electrospinning, including poly lactide-*co*-glycolide (PLGA).[7] Conventional fibers produced by mechanical fiber spinning usually measure tens of microns in diameter, while the submicron-diameter polymeric fibers or nanofibers produced by electrospinning can be readily controlled to provide higher specific surface area and topography that mimics the ECM. Compared to other types of scaffolds, those based on electrospun nanofibers with isotropic aligned fibers have shown superior ability in guiding cell migration,[8] shaping cell morphology,[9] and directing cell differentiation.[10]

Type I collagen (COL I), the basic structural component of bone has been widely investigated and presents excellent properties that facilitate cell attachment.[11,12] Collagen is considered to induce positive effects on cellular adhesion, proliferation and differentiation,[13] and also has direct relevance to orthopedic applications.[14] COL I is used to modify biomaterial surfaces in order to enhance their bioactivity (e.g., on the surfaces of polymers polystyrene,[15] titanium and titanium alloys[16]). However, COL I coated onto the surface has a rapid degradation rate that exceeds the rate of bone regeneration. Similar to other adhesive peptides and growth factors, COL I is immobilized onto biomaterial surfaces via either chemical or physical strategies to avoid rapid degradation.[17,18] Although playing an important role in early cell adhesion and bone mineralization, the function of COL I in such processes is still far from being well-understood.

Mussels have excellent ability to adhere to virtually all types of inorganic and organic surfaces,[19,20] with DOPA and its analogous compounds identified as critical functional elements in the mussel adhesive protein.[21] By self-polymerization of dopamine, a thin polydopamine film can form on the surface of almost all materials.[22] This method has been widely incorporated into glass[23] and organic and polymeric materials,[24,25] such as PLGA[5] and polyethylene glycol (PEG).[26] Because of the presence of catechol and amine functional groups, DOPA increases the hydrophilicity of the cell surface.[27] Studies have shown that the amine group promotes cell adhesion and spreading.[28]

In a dynamic environment, cells respond to chemical and physical stimulation by changing their function or reorganizing the cytoskeleton. Cells interact with the ECM through receptors on their surface, including integrins, which are heterodimeric glycoproteins consisting of α- and β-subunits in mammals. Currently, 18 α and 8 β subunits have been identified and exist in a variety of combinations. Each of these receptors binds to ECM proteins with a different affinity; for example, $\alpha5\beta1$ binds strongly to fibronectin (FN),[29,30] whereas $\alpha1\beta1$, $\alpha2\beta1$, and $\alpha11\beta1$ are known as collagen I receptors. Different integrins regulate the specific behavior of cells; for example, the $\alpha1\beta1$ and $\alpha2\beta1$ integrins have been implicated in the regulation of cell growth and migration in breast cancer.[31] However, the functions of other integrins, such as $\alpha10\beta1$ and $\alpha11\beta1$, in the regulation of cell growth and migration are still unknown. To date, many reports have shown that the topographical and biochemical properties of biomaterials regulate cell adhesion via specific integrins. For example, it has been demonstrated that compared with a smooth surface, the roughness of modified nanoscale surfaces alters the adhesion of erythroleukemia cells by increasing the surface density of adsorbed FN and significantly upregulating $\alpha5\beta1$ mRNA expression.[32] On nanogrooved surfaces, integrins and cell adhesive proteins such as FN or VN (Vitronectin) are also key factors involved in specific cell adhesion.[33] However, the effects of the bioactive properties and topography of interfaces in different stages of adhesion and the interaction with different integrins remain to be clarified.

In this study, four different surfaces were prepared to investigate the roles of topography and bioactive properties on the adhesion and spreading properties of the mouse preosteoblast cell line MC3T3-E1. The PLGA electrospun surface was suitable for the evaluation of cellular adhesion on a surface with a porous rough topography, whereas DOPA and COL I were immobilized to compare the effects of two different bioactive molecules on surfaces. Finally, COL I was immobilized onto a porous electrospun fiber surface (E-COL) to investigate the combined effects of bioactive molecules and topography. Finally, the effects of topography and bioactivity on different stages of adhesion and the expression of specific integrins on the cell morphology, proliferation and $\beta1$ integrin expression were investigated. Analysis of mRNA and protein expression was used for quantitative investigation of integrin-specific responses to topography and bioactivity.

2. MATERIALS AND METHODS

2.1. Preparation of Four Different Surfaces. Five groups: Control, untreated coverslips; DOPA, DOPA-coated coverslips; COL, COL I-coated coverslips; ES, poly lactic-*co*-glycolic acid (PLGA) electrospun fibers; E-COL, COL I immobilized onto ES.

For electrospinning, the PLGA (75/25, 0.72 dL/g inherent viscosity; Jinan Daigang Biomaterial, Jinan, China) was dissolved in trifluoroethanol to a concentration of 10% (w/v). After transferring the polymer solution to a 5 mL glass syringe, the solution was injected in to an infusion pump (TS2−60; Baoding Longer Precision Pump Co. Ltd., Baoding, China) through a stainless-steel blunt needle. The injection rate was 0.4 mL/h under 20 kV voltages (HB-F303−1-AC, Zhejiang, China). Coverslips were adhered to aluminized paper on a flat tray, which was positioned at a distance of 10 cm from the needle tip. The obtained PLGA fibrous membranes (ES) were dried 24 h under vacuum at room temperature.

The type I collagen solution used in this study was prepared according to the previous study.[5] Lyophilized COL was dissolved in 0.05 mol/L acetic acid (China sun Specialty Products, Jiangsu, China) to a concentration of 5 mg/mL. After adjusting the pH to 7.0 with sodium hydroxide solution, the combined and type I collagen surfaces were produced by pouring the type I collagen solution onto the surface of PLGA films and coverslips. The surfaces were rinsed three times with phosphate buffer saline (PBS 1×). Gelation was achieved in approximately 30 min at room temperature followed by evaporation for a further 4 h.

For DOPA surfaces, coverslips were immersed into dopamine (dopamine hydrochloride; Aladdin, Shanghai, China,) solution (2 mg/mL dissolved in 10 mmol/L Tris solution, pH 8.5). After self-polymerization for 24 h, a nanoscale thin polydopamine (PDA) film

Table 1. Primers for RT-PCR Analysis

gene	forward primer (5′-3′)	reverse primer (5′-3′)
β1 Integrin	ATCCCAATTGTAGCAGGCGTGGTT	GACCACAGTTGTCACGGCACTC
α1 Integrin	CTGCTGCCTGTGGACTTTAG	CTGGAGCGGTGGAAGAGTAA
α2 Integrin	GGGACCTCACAAACACCTTC	ACTGCTATGCCGAACCTCAG
α5 Integrin	GGGAGTGAGACCTGGCAACT	CTGGAGCGGTGGAAGAGTAA
α10 Integrin	TTGTGAGAGCAGCAAGGAAC	TAGTGACCAAGGACCGCAAT
α11 Integrin	AGGATGGGCTTGTGGACCTA	GACGGTTGCTGTTTGGAAGT
gapdh	TGCACCACCAACTGCTTAGC	GTCTTCTGGGTGGCAGTGATG

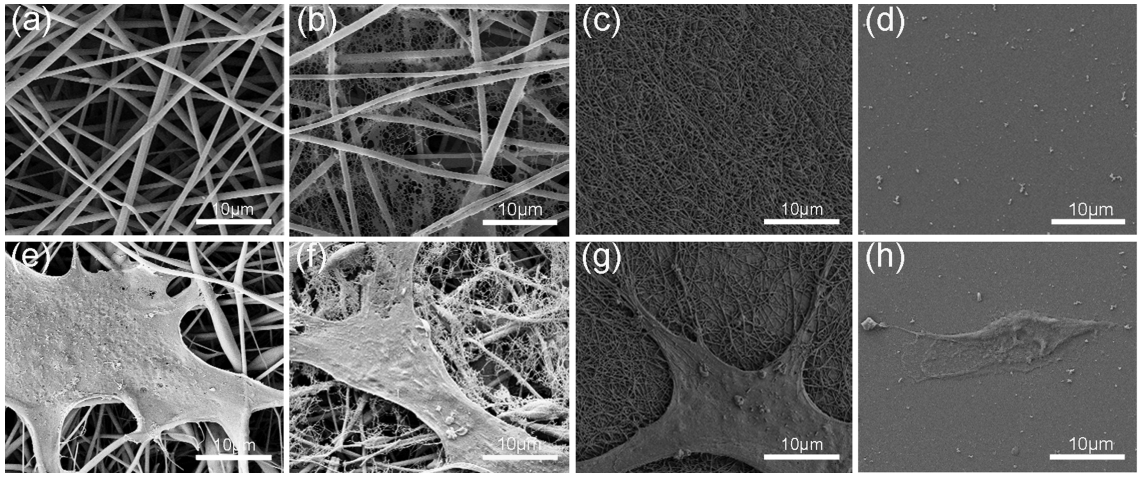

Figure 1. Field-emission scanning electron microscopy images of different surfaces and MC3T3-E1 cell morphologies at 12 h after seeding on different surfaces (Control, untreated coverslips; DOPA, DOPA-coated coverslips; COL, COL I-coated coverslips; ES, poly lactic-*co*-glycolic acid (PLGA) electrospun fibers (ES); E-COL, COL I immobilized onto ES). (a, e) ES surface; (b, f) E-COL surface; (c, g): COL surface; (d, h) DOPA surface.

formed on the surface of the coverslips. The PDA coverslips were rinsed three times with Tris solution.

All procedures were performed using aseptic technique and the prepared surfaces were sterilized under UV for 4 h before cell-seeding.

2.2. Cell Culture. The MC3T3-E1 cell line (subclone 14) was purchased from the Cell Bank of the Chinese Science Academy (Shanghai, China). Cells were cultured in a complete medium containing α-modified minimum essential medium (α-MEM; HyClone, Logan, UT, USA) supplemented with 10% fetal bovine serum (Hyclone), 100 mg/mL streptomycin, and 100 U/ml penicillin (Beyotime, Shanghai, China). After reaching 80−90% confluence, the cells were detached using 0.25% trypsin (Gibco, NY, USA) containing ethylenediaminetetraacetic acid (EDTA) and counted with a hemocytometer. Cells were subcultured at least twice a week and were maintained at a humidified atmosphere of 95% air and 5% CO_2. Cells below passage 20 were used for this study.

2.3. Cell Proliferation. Cell Counting Kit-8 Cells used for seeding the surfaces were plated in a 24-well plate at a density of 8×10^3 cells/well in triplicate. At 1, 3, 5, 7, and 9 days after seeding, the cell viability was measured using CCK-8 (Cell Counting Kit-8; Beyotime) assays according to the manufacturers' instructions. The optical density (OD) at 450 nm was determined via an enzyme-linked immunosorbent assay plate reader (Titertek, Helsinki, Finland). Three independent experiments were performed for each assay condition.

Flow cytometry (FCM) was used to further evaluate the cell cycle. Cells were seeded in the different groups at a concentration of 3×10^4/mL and synchronized by serum-starvation for 24 h. At day 5 after synchronization, the cells were collected, washed three times in ice-cold PBS (pH 7.4) and fixed in ice-cold 70% ethanol for storage at −20 °C overnight. Cells were incubated with 0.1 mg/mL RNase for 30 min at 37 °C, and stained with 50 μg/mL PI (Sigma, St. Louis, USA). The cell cycle was investigated by FCM (BD FACSCalibur, San Jose, CA) and further analyzed for cell cycle distribution using Cell Quest software. The cell cycle distributions (G_1, S, and G_2/M phases) were described and compared. The experiment was repeated in triplicate.

2.4. Cell Attachment. The morphology of cells that adhered to the surfaces were visualized after cultivation for 6, 12, and 24 h using confocal laser scanning microscopy (CLSM; Zeiss-LSM710; Carl Zeiss, Inc., Jena, Germany) and field-emission scanning electron microscopy (FESEM; S-4800; Hitachi, Tokyo, Japan).The cells were seeded as described in Section 2.3.

For CLSM, the samples were washed with PBS (1×), fixed with 3.7% paraformaldehyde for 30 min at room temperature and then permeabilized with 0.25% Triton X-100/PBS for 3 min. Cells were then incubated with rhodamine phalloidin (1:200 dilution; Cytoskeleton, Inc., Denver, CO, USA) for 30 min and rinsed five times with PBS (1×). After incubation with 4′, 6-diamidino-2-phenylindole (DAPI, Beyotime) (1:2000 dilution) for 30 s in the dark at room temperature, samples were rinsed fives times with PBS (1×) and observed by CLSM.

For FESEM, samples were fixed with 2.5% glutaraldehyde (pH 7.4) for 4 h, dehydrated using a gradient series of ethanol:distilled water (30:70, 50:50, 90:10, and 100:0). Each sample was freeze-dried under vacuum and sputter-coated with gold for observation by FESEM.

2.5. Integrin β1 Immunofluorescence. After cultivation for 6, 12, and 24 h, the samples were rinsed with PBS (1×), fixed with 3.7% paraformaldehyde for 15 min at room temperature, permeabilized with 0.5% Triton X-100 in PBS for 3 min and sequentially blocked with 3% bovine serum albumin (BSA) for 30 min. Following overnight incubation with the specific primary detection antibody (β1, Abcam plc,) (1:50 dilution), cells were further incubated with the secondary antibody, Alexa Fluor 488 goat antirabbit IgG (Beyotime) (1:200 dilution), and cytoskeleton actin staining (Inc.). Images were captured using a Zeiss LSM 710 microscope and analyzed using the LSM image browser.

2.6. RNA Isolation and RT-PCR. Cells were centrifuged at 1000 rpm for 5 min and total RNA was extracted using the TRIzol reagent

(Invitrogen) following the manufacturer's protocol. Reverse transcription reactions were performed with 1000 ng total RNA using PrimeScript RT reagent kit (TaKaRa Bio Co., Ltd., Otsu, Japan). The generated cDNA was used as template for real-time PCR reactions using SYBR Premix Ex Taq kit (TaKaRa). The sequences of primers used in this study are listed in Table 1. Real-time PCR reactions were performed using the ABI 7300 Real-time PCR System (Applied Biosystems, USA) using the following conditions: 95 °C for 5 min, followed by 40 cycles of amplification, consisting of a denaturation step at 95 °C for 10 s, and an extension step at 60 °C for 31 s. The level of expression of the target gene, normalized to glyceralde-hyde-3-phosphate dehydrogenase (GAPDH). Relative gene expression values were calculated by the $2^{\Delta\Delta Ct}$ method as previously described.[34] The experiment was performed three times.

2.7. Western Blot Analysis. Cells were centrifuged at 1000 rpm for 5 min. Total protein was extracted from cells using RIPA and 1% Pheylmethylsulfonyl fluoride (PMSF, Shenergy Biocolor, China). The supernatant was collected following centrifugation for 5 min at 12 000*g* (4 °C). The protein concentration was assessed using a Bradford method. Equal amounts of protein samples were separated by 10% SDS-PAGE and transferred onto polyvinylidene fluoride (PVDF) membranes (Millipore, Massachusetts, USA) membranes. The membranes were then blocked in Tris-buffered saline with 0.1% Tween-20 (TBST), containing 5% skimmed milk for 2 h at room temperature. The blocked membranes were then incubated with primary antibody Integrin β1 (Abcam) (1:800 dilution) at 4 °C overnight. GAPDH (Bioworld, USA) was used as an internal control. After washing with TBST the next day, membranes were incubated in PBS, containing the secondary antibody (horseradish peroxidase goat antirabbit conjugated, Beyotime, Shanghai, China) (1:2000 dilution) at room temperature for 1 h. Immunoreactive bands were detected using the enhanced chemiluminescence reagent (Millipore). Western blot results were analyzed using the ImageJ (NIH, Bethesda, USA) and GraphPad Prime 5.0 software. Each experiment was performed for three times.

2.8. Statistical Analysis. Statistical analysis was performed using SPSS v.17.0 software. Data were presented as the mean ± SD. Significance was accepted at a level of $P < 0.05$. After testing the data for normality, statistical analysis was performed using one-way ANOVA followed by the least significant difference test (LSD). All quantitative data reported represent the mean of at least three independent experiments.

3. RESULTS AND DISCUSSION

3.1. Microstructure of Different Surfaces. FESEM images of the different surfaces are shown in Figure 1. Uniform and smooth PLGA electrospun (ES) fibers (diameter, 500 nm to 1 μm) were randomly arranged, forming rough surfaces containing interconnected pores (Figure 1a). In contrast to ES, E-COL exhibited a spider-web-like topography that penetrated throughout the interconnected pores (Figure 1b). The topographies of the COL and DOPA surfaces were distinct (Figure 1c, d). The bundles of COL I fibers in COL were irregular in arrangement (Figure 1c), whereas DOPA showed a relatively smooth surface (Figure 1d). At 12 h after seeding on the different surfaces, cells appeared well-spread in all groups. In the ES and E-COL groups, cells were anchored to the surface via filopodia along the electrospun fibers (Figure 1e, f), whereas the filopodia of cells in the COL group were intertwined with the collagen fibers (Figure 1g). The large specific surface area and high length to diameter ratio of electrospun fibers in the ES group facilitates the diffusion of fluids, oxygen and bioactive substances for cell growth, which is vital for bone regeneration. The roughness of the electrospun fibers is suitable for COL I immobilization, and increases the cell contact area. Furthermore, because of the immobilization of the bioactive material, E-COL may possess a better bioactivity than ES. On the DOPA surface, cells showed different shape with no obvious lamellipodia than the ES, E-COL and COL surfaces (Figure 1h).

3.2. Cell Attachment Analysis. A suitable interface for bone regeneration must be biocompatible for cell attachment. The cellular adhesion process is adjusted by the interaction of the cell with the ECM, resulting in the formation of focal adhesions and organization of the cytoskeleton.[35] The cytoskeleton is a three-dimensional grid structure composed of a variety of specific proteins, which is important for maintaining cell differentiation, migration and exercising systolic functions.[36] Cellular morphology on different surfaces was compared (Figure 2). Compared to serum-free conditions,

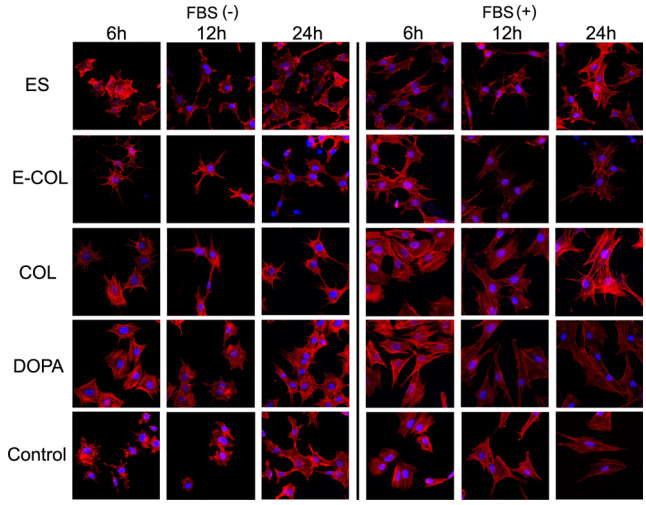

Figure 2. Confocal laser scanning microscopy images (×400) of morphology of cells cultured on different surfaces (Control, untreated coverslips; DOPA, DOPA-coated coverslips; COL, COL I-coated coverslips; ES, poly lactic-*co*-glycolic acid (PLGA) electrospun fibers (ES); E-COL, COL I immobilized onto ES). Cells were immunostained for F-actin (red) and nucleus (blue). FBS (−): cells cultured in serum-free medium. FBS (+): cells cultured in serum medium. Cell adhesion on different surfaces was compared by cellular morphology.

cells cultured under serum-containing conditions presented a larger cell spreading area with fully stretched pseudopodia, indicating that cells attachment is facilitated under these conditions. It can be speculated that ECM proteins, including FN, obtained from serum are adsorbed to the surface allowing direct interaction with cells.[37] At 6 and 12 h after seeding under serum-free conditions, the cytoskeleton was well-organized in the E-COL, COL and DOPA groups, with long, thin filopodia present in the COL and DOPA groups. However, the actin filaments on the ES or Control surfaces were disordered. Our results indicate that bioactive molecules play an important role in cell adhesion under serum-free conditions; however the topography of surfaces does not appear to modify cell adhesion behavior. In the serum-containing environment, numerous well-defined and small filopodia were observed on the ES and E-COL surfaces at 6 h after seeding, especially on the E-COL surface, indicating enhanced biocompatibility. Cells on the control surfaces presented a round shape with no obvious pseudopodia. At 12 and 24 h after seeding, the cells exhibited a well-spread shape, with a well-organized cytoskeleton observed in all groups. These results indicate that the topography of the surface plays an important role in the early stages of cell

adhesion. Compared with the effects of any of the topographic or bioactive properties in isolation, the combined effects of the two types of properties provided an advantage in cell adhesion and spreading, possibly because of enhanced protein adsorption induced by the increased roughness or specific surface area.

3.3. Integrin β1 Immunofluorescence Analysis. Immunofluorescence studies were conducted to investigate the role of β1 integrin molecules in cell attachment (Figure 3). This

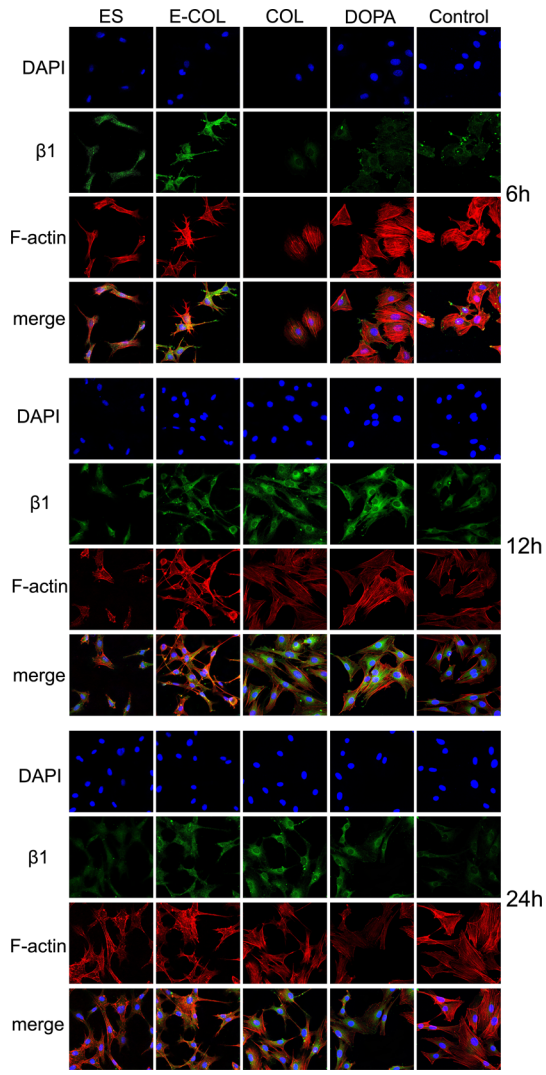

Figure 3. Localization of β1 integrin and F-actin protein was identified by immunofluorescence staining at 6, 12, and 24 h after seeding onto the different surfaces (Control, untreated coverslips; DOPA, DOPA-coated coverslips; COL, COL I-coated coverslips; ES, poly lactic-*co*-glycolic acid (PLGA) electrospun fibers (ES); E-COL, COL I immobilized onto ES). Cells were observed by confocal laser scanning microscopy (× 200) and immunostained for F-actin (red), nucleus (blue), β1 (green). The bottom rows in each panel show the merged images.

is an essential transmembrane molecule, which acts as a link between the extracellular matrix and cytoskeleton proteins.[38] In our study, after seeding for 6, 12, and 24 h in a serum-containing environment, cells cultured on all surfaces expressed β1 integrin protein. As shown in Figure 3, the distribution of β1 was in accordance with cell morphology and localized at the plasma membrane. At 6 h, the cells presented a round shape with almost no spreading in COL, DOPA and Control groups. High expression of β1 integrin was detected in the E-COL group, whereas there was almost no expression in the other four groups. Elongated pseudopodia were observed in the E-COL and ES groups, whereas no obvious pseudopodia were observed in the other groups. However, at 12 and 24 h, high expression of β1 integrin was observed in all groups. Previous studies have indicated that β1 integrin expression facilitates the attachment of cells onto the surface by mediateing the interaction between cells and adsorbed matrix proteins from the culture medium.[39] Our results indicate that proteins are adsorbed onto the biomaterial surface via topographic properties in the early stages of adhesion, which is consistent with the CLSM results. The distribution of β1 integrin was almost identical to that of the actin cytoskeleton. Studies have shown that cell movement and differentiation are regulated by the actin cytoskeleton in a process that may involve integrin-mediated matrix binding and signaling pathways,[40,41]

3.4. Western Blot and RT-PCR Analyses of β1 Integrin Expression. It is now widely acknowledged that integrins act as cell adhesion molecule bind to ECM proteins regulating intracellular signaling and facilitating cell attachment and spreading.[42] In this study, a quantitative analysis of β1 expression and that of the α subunits was then conducted to investigate the involvement of different adhesion receptors during the adhesion process.

The mRNA and protein expression levels of the β1 subunit were measured quantitatively by RT-PCR and Western blot analyses, respectively (Figure 4). At 6 h after seeding, β1 integrin mRNA expression of cells grown on E-COL was obviously upregulated compared with the other groups ($P < 0.05$) (Figure 4a). Furthermore, increased β1 integrin mRNA expression was observed in the COL and DOPA groups in comparison with the Control group at 12 h ($P < 0.05$) (Figure 4b), whereas there were no significant changes in expression in any of the groups at 24 h ($P > 0.05$) (Figure 4c). Combined with the CLSM results, this finding suggests that both the topography and bioactive characteristics modulate β1 integrin mRNA expression in the early stages of adhesion and that this effect is enhanced by the combination of the two characteristics.

At 6 h, β1 integrin protein expression in the cells grown on E-COL was significantly higher than those in the other four groups ($P < 0.01$) (Figure 4d). In addition, at 6 h, higher levels were detected in the ES group compared with those in the DOPA, COL and Control groups ($P < 0.05$) (Figure 4d). These results suggest that the rough topography may significantly modulate β1 integrin expression in the early stages of adhesion, while bioactive characteristics play an important role at the later stages. At 12 and 24 h, β1 integrin protein levels were consistent with the mRNA levels detected by RT-PCR. At 12 h, the β1 integrin protein levels in the DOPA and COL groups were significantly upregulated compared with that in the Control group ($P < 0.01$) (Figure 4e). β1 protein expression in the E-COL group was significantly higher than that in the other four groups ($P < 0.001$). These results further suggest that the topographical properties of the surface play an important role in regulating the expression β1 integrin in the early stages, whereas the combined effect of topographical and bioactive characteristics exert a greater effect that either of the individual types of characteristics alone. It may be that collagen fibers in two-dimensions offer a high degree of polymerization and tight arrangement, whereas the distribution of the three-dimensional space between the electrospun fibers exposes more collagen active sites than the two-dimensional arrangement. However,

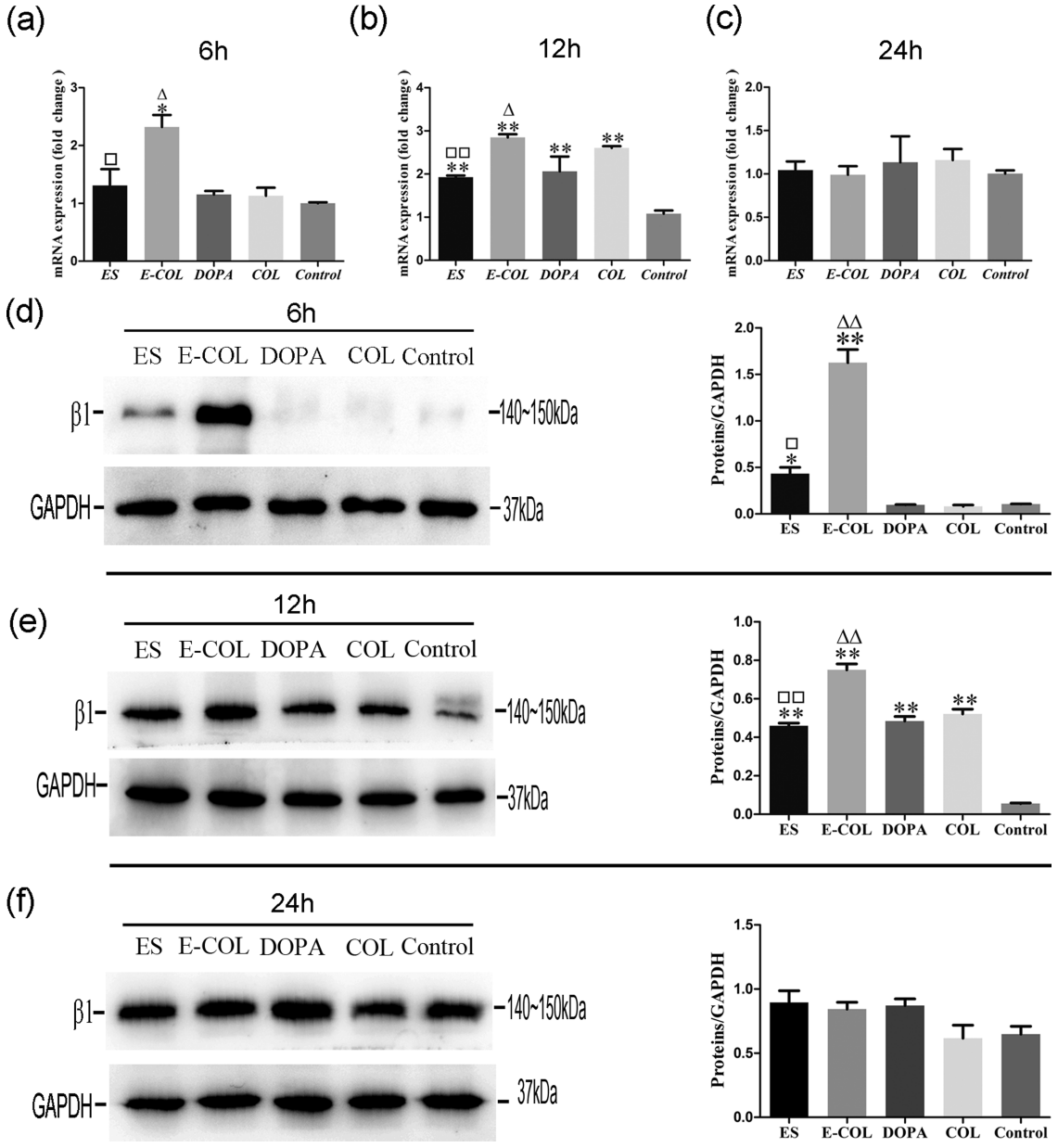

Figure 4. (a–c) Gene expression levels of β1 integrin relative to gapdh in cells cultured on different surfaces. d–f: Protein expression levels of integrin β1 relative to GAPDH in cells cultured on the five surfaces (Control, untreated coverslips; DOPA, DOPA-coated coverslips; COL, COL I-coated coverslips; ES, poly lactic-*co*-glycolic acid (PLGA) electrospun fibers (ES); E-COL, COL I immobilized onto ES) (left). Densitometry analysis of each band was performed and calculated using GAPDH expression as a control (right). *, $P < 0.05$ vs Control; Δ, $P < 0.05$ vs COL; □, $P < 0.05$ vs E-COL.

there were no significant differences in β1 integrin expression of the different groups at 24 h ($p > 0.05$) (Figure 4f). We hypothesize that this is due to adsorption of proteins from the serum. At 6 h, protein adsorption by rough surfaces was more rapid than that of bioactive sufaces, thus providing an adhesion advantage. However, at 24 h, adsorption of proteins was complete so there was no significant difference in integrin expression levels between the groups.

3.5. RT-PCR Analysis of α-Integrin Subunits. Integrins bind specifically to the proteins adsorbed on surface of materials, acting as a bridge between the cell and the ECM.[43,44] Integrins comprise an α chain and a β chain; two transmembrane glycoprotein subunits, which are noncovalently bound. The most common binding site is the tripeptide amino acid sequence arginine–glycine–aspartic acid (RGD),[45,46] which is present in most ECM proteins, such as FN, VN and the collagens. However, several other restricted recognition sequences, for instance, the DGEA (Asp–Gly–Glu–Ala) sequence in collagen I are also recognized by $\alpha 2\beta 1$ integrin, and blocking ECM proteins or integrins with antibodies proved significant inhibition of cell adhesion and spreading.[39,47] Previous studies have demonstrated that $\alpha 1/\beta 1$, $\alpha 2/\beta 1$, $\alpha 10/\beta 1$, and $\alpha 11/\beta 1$ are major receptors for collagen, whereas $\alpha 5$ is known as a specific FN-binding integrin.[48] Figure 5 shows the α-integrin gene ($\alpha 1$, $\alpha 2$, $\alpha 5$, $\alpha 10$, and $\alpha 11$) expression in the cells cultured on the five different surfaces at 6, 12, and 24 h after seeding. Our data showed that $\alpha 5$ integrin gene expression was significantly upregulated in the DOPA group at the 12 and 24 h compared with the levels in the other groups ($P < 0.001$). Combined with the obvious changes in cell morphology

dx.doi.org/10.1021/am5047944 | ACS Appl. Mater. Interfaces 2014, 6, 17134–17143

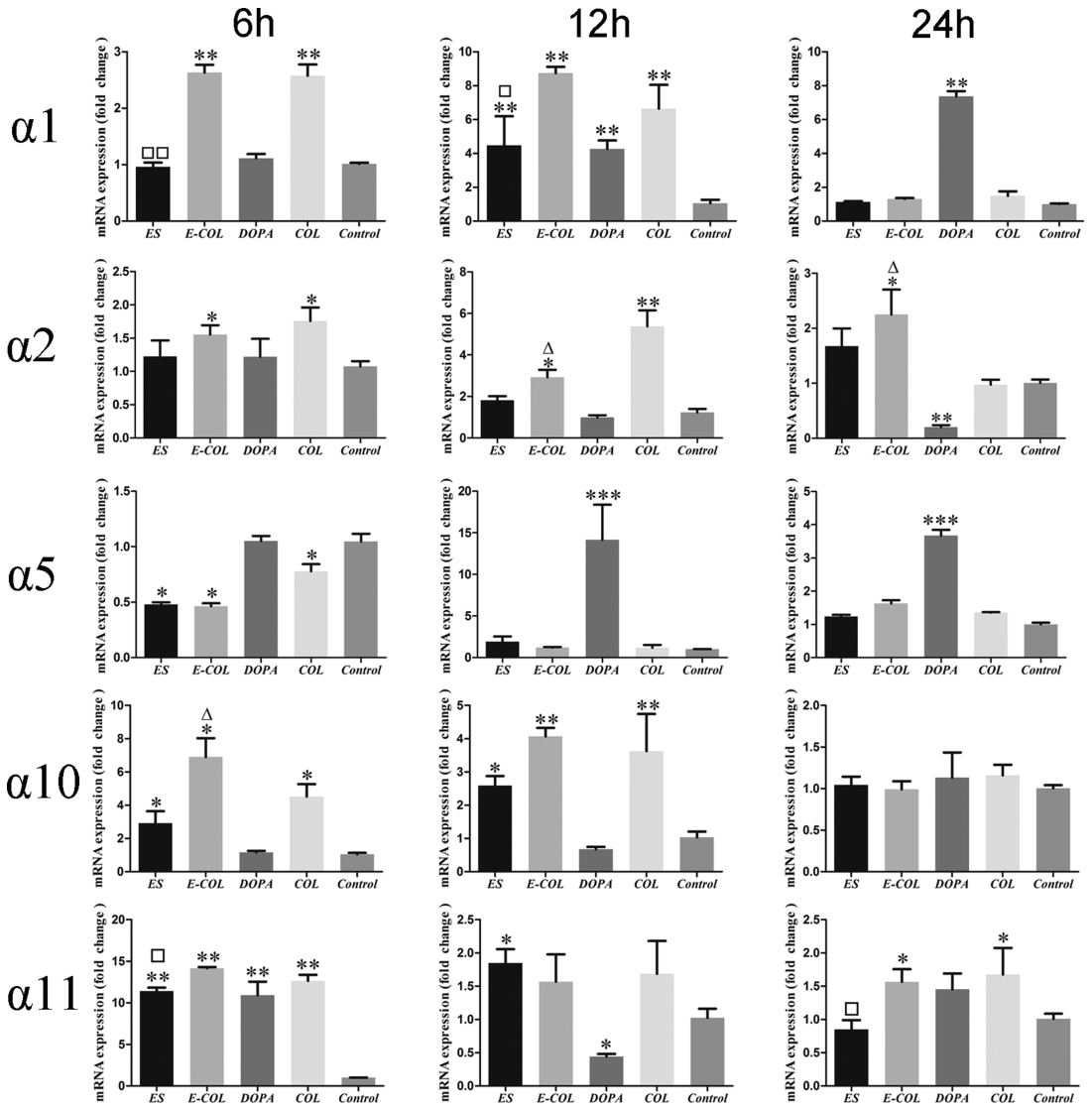

Figure 5. Gene expression levels of different integrins (α1, α2, α5, α10, α11) relative to gapdh in cells at 6, 12, and 24 h after seeding on different surfaces. Densitometry analysis of each band was performed and calculated using GAPDH expression as a control. *, $P < 0.05$ vs Control; Δ, $P < 0.05$ vs COL; □, $P < 0.05$ vs E-COL.

observed in the DOPA group, our results indicate that DOPA acts primarily by adsorbing FN from the serum to increase the adhesion. Investigations have shown that the surface free energy of materials is obviously increased after coating with DOPA, which is widely used as an intermediate layer for covalent immobilization of bioactive molecules such as heparin and BSA.[49] However, collagen I is highly polymerized, forming fibers in the COL surface, which may inhibit optimal binding of bioactive molecules from the serum by steric hindrance. Thus, it can be speculated that FN adsorption to the COL surface was less efficient than to the DOPA surface. Study revealed that immobilization onto the surface of biomaterials allows FN to mediate bone morphogenesis and differentiation of osteoblasts via $\alpha5/\beta1$.[32] At 6 and 12 h the gene expression of α1, α2, α10, and α11 integrins was significantly upregulated in the COL and E-COL groups compared with the levels in the other groups ($P < 0.05$) (Figure 5). It may be that binding sites such as the RGD and DGEA sequences on the COL surface are recognized by the integrins. It was in consistent with the previous study.[50] However, at 24 h, there were no significant differences between the groups ($P > 0.05$).

Expression of α1 was significantly upregulated in the E-COL group compared with that in the COL group at 12 h ($P < 0.05$). Compared with the Control group, α10 expression was significantly upregulated in the ES group at 6 and 12 h ($P < 0.05$), whereas α11 expression in this group was significantly upregulated at 6 h ($P < 0.05$). These observations indicate that the topography of surfaces plays an important role in the early stages via mediating the expression of α1, α10, and α11. Various studies have demonstrated that surface roughness and porous topography contribute to the adsorption of organic substances from the serum, which could enhance the initial attachment of cells compared with a smooth surface.[51,52] Electrospun fibers are thought to bear physical similarity to natural collagen or the ECM.[53,54] The porosity of electrospun surfaces can facilitate nutrient transport, such as fluids, oxygen and bioactive substances. It can be speculated that organic substances adsorbed from the serum upregulate the expression of α1, α10, and α11 in the early stages of adhesion although this requires further investigation. Thus, our data show that surface topography promotes α1, α10, and α11 expression at 6 h, whereas the expression of α2 was not correlated with surface

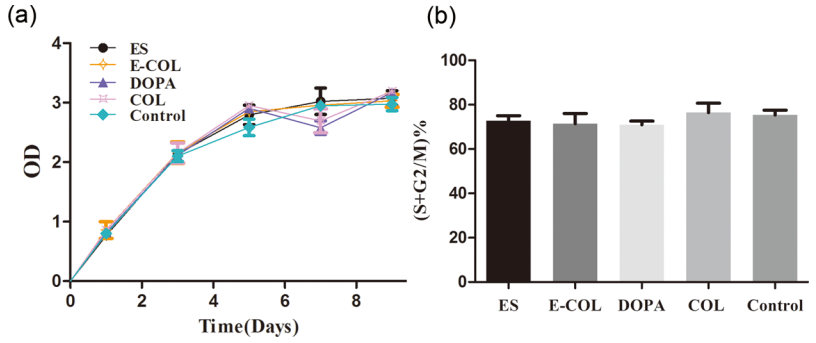

Figure 6. (a) Proliferation of cells seeded on different surfaces measured using CCK-8 assays (n = 3, P > 0.05). (b) Flow cytometric analysis of the cell cycle distribution among cells seeded on different surfaces at day 5 (n = 3, P > 0.05). (S + G2/M) % means proliferation index. Control, untreated coverslips; DOPA, DOPA-coated coverslips; COL, COL I-coated coverslips; ES, poly lactic-*co*-glycolic acid (PLGA) electrospun fibers (ES); E-COL, COL I immobilized onto ES. No statistical differences were detected between groups at the same time point in CCK-8 assays and flow cytometric analysis.

topography. This result confirms that the influence of surface topography on integrin expression is variable.

3.6. Cell Proliferation. After cells adhere to the materials, a series of processes including proliferation, differentiation, and ECM deposition continue to occur.[55,56] Cell proliferation on different surfaces was analyzed in Cell Counting Kit-8 assay (CCK-8) and FCM assays (Figure 6). In CCK-8 assays, generally increasing OD levels were observed from 1 to 9 d in all groups, indicating a good biocompatibility for cell proliferation in all groups, with no statistical differences detected between different surfaces at same time point (P > 0.05) (Figure 6a). These results were confirmed by FCM analysis. Flow cytometry assay revealed that the percentage of cells in S and G2/M phases were not significantly different when detected between different surfaces at 5 days (P > 0.05) (Figure 6b). Western blot and real-time RT-PCR analyses indicated that the topography and bioactive components of surfaces significantly affect cell adhesion in the early stages, while these features did not influence cell proliferation at later stages. Studies have shown that the interaction of integrins with the ECM affect osteoblast expression of transcription factors and osteoblast-specific genes.[57,58] A previous study revealed that adhesion and osteogenic differentiation of bone marrow-derived mesenchymal stems was promoted in culture on DOPA-coated surfaces, while apoptosis was not affected.[59] We hypothesize that topographic and bioactive modifications of surfaces influence the later stages of osteogenic differentiation of cells via integrin molecule interactions. In addition, Cellular proliferation may be affected by many other factors, such as three-dimensional space and sufficient nutrition; however, further studies on the influence of topographic and bioactive modifications of biomaterials on osteoblast differentiation and proliferation are required.

CONCLUSIONS

In this study, we developed four different surfaces to investigate the role of surface topography and biological properties in regulating cellular behavior. PLGA electrospun fibers were produced for to generate a porous rough surface, whereas DOPA and type I collagen were immobilized to coverslips to provide different bioactive surfaces. Type I collagen-coated PLGA electrospun fibers were used to investigate the combined effects of bioactive molecules and topography on the adhesion and growth behavior of preosteoblast MC3T3-E1 cells. Immunofluorescence analysis of cell morphology indicated that surface topography plays an important role in regulating the early stages of cell adhesion. Furthermore, RT-PCR and Western blot analyses demonstrated that the combined effect of topographical and bioactive characteristics exerts a greater effect than that of either of the individual types of characteristics alone. This study provides new insights into the functions and effects of topographic and bioactive modifications of surfaces at the interface between cells and biomaterials for tissue engineering.

AUTHOR INFORMATION

Corresponding Author

*E-mail: fmzhang@njmu.edu.cn.

Author Contributions

The manuscript was written through contributions of all authors. All authors have given approval to the final version of the manuscript.

Funding

This work was supported by grants from the Outstanding Medical Academic Leader Program and Creative team of Jiangsu Province, the Priority Academic Program Development of Jiangsu Higher Education Institutions (PAPD, 2014−37). National Natural Science Foundation of China (31200757 and 81400486), Natural Science Foundation of Jiangsu Province (20140911), and Science and Technology Project in Suzhou (SYG201210).

Notes

The authors declare no competing financial interest.

ACKNOWLEDGMENTS

The authors express their gratitude to Yan Fang (Nanjing Institute of Geology and Palaeontology, Chinese Academy of Sciences) for his help in FESEM analysis.

REFERENCES

(1) Wang, X.; Ma, J.; Wang, Y.; He, B. Bone Repair in Radii and Tibias of Rabbits with Phosphorylated Chitosan Reinforced Calcium Phosphate Cements. *Biomaterials* **2002**, *23*, 4167−4176.

(2) Murugan, R.; Ramakrishna, S. Nano-featured Scaffolds for Tissue Engineering: a Review of Spinning Methodologies. *Tissue Eng.* **2006**, *12*, 435−447.

(3) Jahani, H.; Kaviani, S.; Hassanpour-Ezatti, M.; Soleimani, M.; Kaviani, Z.; Zonoubi, Z. The Effect of Aligned and Random Electrospun Fibrous Scaffolds on Rat Mesenchymal Stem Cell Proliferation. *Cell* **2012**, *14*, 31−38.

(4) Ko, E.; Yang, K.; Shin, J.; Cho, S. W. Polydopamine-assisted Osteoinductive Peptide Immobilization of Polymer Scaffolds for Enhanced Bone Regeneration by Human Adipose-derived Stem Cells. *Biomacromolecules* **2013**, *14*, 3202−3213.
(5) Chen, G.; Xia, Y.; Lu, X.; Zhou, X.; Zhang, F.; Gu, N. Effects of Surface Functionalization of PLGA Membranes for Guided Bone Regeneration on Proliferation and Behavior of Osteoblasts. *J. Biomed Mater. Res. Part A* **2013**, *101*, 44−53.
(6) Shin, S. H.; Purevdorj, O.; Castano, O.; Planell, J. A.; Kim, H. W. A Short Review: Recent Advances in Electrospinning for Bone Tissue Regeneration. *J. Tissue Eng.* **2012**, *3*, 2041731412443530.
(7) Agarwal, S.; Wendorff, J. H.; Greiner, A. Progress in the Field of Electrospinning for Tissue Engineering Applications. *Adv. Mater.* **2009**, *21*, 3343−3351.
(8) Schnell, E.; Klinkhammer, K.; Balzer, S.; Brook, G.; Klee, D.; Dalton, P.; Mey, J. Guidance of Glial Cell Migration and Axonal Growth on Electrospun Nanofibers of Poly-Epsilon-Caprolactone and a Collagen/Poly-Epsilon-Caprolactone Blend. *Biomaterials* **2007**, *28*, 3012−3025.
(9) Hashi, C. K.; Zhu, Y.; Yang, G. Y.; Young, W. L.; Hsiao, B. S.; Wang, K.; Chu, B.; Li, S. Antithrombogenic Property of Bone Marrow Mesenchymal Stem Cells in Nanofibrous Vascular Grafts. *Proc. Natl. Acad. Sci. U.S.A.* **2007**, *104*, 11915−11920.
(10) Li, D.; Sun, H.; Jiang, L.; Zhang, K.; Liu, W.; Zhu, Y.; Fangteng, J.; Shi, C.; Zhao, L.; Yang, B. Enhanced Biocompatibility of PLGA Nanofibers with Gelatin/Nano-Hydroxyapatite Bone Biomimetics Incorporation. *ACS Appl. Mater. Interfaces* **2014**, *6*, 9402−9410.
(11) Madhavan, K.; Belchenko, D.; Motta, A.; Tan, W. Evaluation of Composition and Crosslinking Effects on Collagen-based Composite Constructs. *Acta biomater* **2010**, *6*, 1413−1422.
(12) Wang, L.; Stegemann, J. P. Glyoxal Crosslinking of Cell-seeded Chitosan/Collagen Hydrogels for Bone Regeneration. *Acta Biomater.* **2011**, *7*, 2410−2417.
(13) Kleinman, H. K.; Klebe, R. J.; Martin, G. R. Role of Collagenous Matrices in the Adhesion and Growth of Cells. *J. Cell Biol.* **1981**, *88*, 473−485.
(14) LeBaron, R. G.; Athanasiou, K. A. Extracellular Matrix Cell Adhesion Peptides: Functional Applications in Orthopedic Materials. *Tissue Eng.* **2000**, *6*, 85−103.
(15) Fischer, B. E.; Thomas, K. B.; Dorner, F. Collagen Covalently Immobilized onto Plastic Surfaces Simplifies Measurement of Von Willebrand Factor-Collagen Binding Activity. *Ann. Hematol.* **1998**, *76*, 159−166.
(16) Geissler, U.; Hempel, U.; Wolf, C.; Scharnweber, D.; Worch, H.; Wenzel, K. W. Collagen Type I-coating of Ti6Al4V Promotes Adhesion of Osteoblasts. *J. Biomed. Mater. Res.* **2000**, *51*, 752−760.
(17) Ito, Y.; Liu, S. Q.; Imanishi, Y. Enhancement of Cell Growth on Growth Factor-immobilized Polymer Film. *Biomaterials* **1991**, *12*, 449−453.
(18) Masters, K. S. Covalent Growth Factor Immobilization Strategies for Tissue Repair and Regeneration. *Macromol. Biosci* **2011**, *11*, 1149−1163.
(19) Ku, S. H.; Lee, J. S.; Park, C. B. Spatial Control of Cell Adhesion and Patterning Through Mussel-inspired Surface Modification by Polydopamine. *Langmuir* **2010**, *26*, 15104−15108.
(20) Lee, H.; Scherer, N. F.; Messersmith, P. B. Single-molecule Mechanics of Mussel Adhesion. *Proc. Natl. Acad. Sci. U.S.A.* **2006**, *103*, 12999−13003.
(21) Silverman, H. G.; Roberto, F. F. Understanding Marine Mussel Adhesion. *Mar. Biotechnol.* **2007**, *9*, 661−681.
(22) Saxer, S.; Portmann, C.; Tosatti, S.; Gademann, K.; Zurcher, S.; Textor, M. Surface Assembly of Catechol-Functionalized Poly(L-lysine)-Graft-Poly(ethylene glycol) Copolymer on Titanium Exploiting Combined Electrostatically Driven Self-organization and Biomimetic Strong Adhesion. *Macromolecules* **2010**, *43*, 1050−1060.
(23) Zhang, W.; Yang, F. K.; Han, Y.; Gaikwad, R.; Leonenko, Z.; Zhao, B. Surface and Tribological Behaviors of the Bioinspired Polydopamine Thin Films under Dry and Wet Conditions. *Biomacromolecules* **2013**, *14*, 394−405.
(24) Tahir, M. N.; Zink, N.; Eberhardt, M.; Therese, H. A.; Kolb, U.; Theato, P.; Tremel, W. Overcoming the Insolubility of Molybdenum Disulfide Nanoparticles through a High Degree of Sidewall Functionalization Using Polymeric Chelating Ligands. *Angew. Chem., Int. Ed. Engl.* **2006**, *45*, 4809−4815.
(25) Ye, Q.; Zhou, F.; Liu, W. Bioinspired Catecholic Chemistry for Surface Modification. *Chem. Soc. Rev.* **2011**, *40*, 4244−4258.
(26) Ai, Y.; Wei, Y.; Nie, J.; Yang, D. Study on the Synthesis and Properties of Mussel Mimetic Poly(ethylene glycol) Bioadhesive. *J. Photochem. Photobiol., B* **2013**, *120*, 183−190.
(27) Kim, B. J.; Choi, Y. S.; Choi, B. H.; Lim, S.; Song, Y. H.; Cha, H. J. Mussel Adhesive Protein Fused with Cell Adhesion Recognition Motif Triggers Integrin-mediated Adhesion and Signaling for Enhanced Cell Spreading, Proliferation, and Survival. *J. Biomed. Mater. Res. Part A* **2010**, *94*, 886−892.
(28) Zimmermann, C. E.; Gierloff, M.; Hedderich, J.; Acil, Y.; Wiltfang, J.; Terheyden, H. Survival of Transplanted Rat Bone Marrow-derived Osteogenic Stem Cells in Vivo. *Tissue Eng., Part A* **2011**, *17*, 1147−1156.
(29) Obara, M.; Kang, M. S.; Yamada, K. M. Site-directed mutagenesis of the cell-binding domain of human fibronectin: separable, synergistic sites mediate adhesive function. *Cell.* **1988**, *53*, 649−657.
(30) Aota, S.; Nomizu, M.; Yamada, K. M. The short amino acid sequence Pro-His-Ser-Arg-Asn in human fibronectin enhances cell-adhesive function. *J. Biol. Chem.* **1994**, *269*, 24756−24761.
(31) Lindberg, K.; Strom, A.; Lock, J. G.; Gustafsson, J. A.; Haldosen, L. A.; Helguero, L. A. Expression of Estrogen Receptor Beta Increases Integrin alpha1 and Integrin beta1 Levels and Enhances Adhesion of Breast Cancer Cells. *J. Cell. Physiol.* **2010**, *222*, 156−167.
(32) Lee, M. H.; Ducheyne, P.; Lynch, L.; Boettiger, D.; Composto, R. J. Effect of Biomaterial Surface Properties on Fibronectin-alpha5beta1 Integrin Interaction and Cellular Attachment. *Biomaterials* **2006**, *27*, 1907−1916.
(33) Lamers, E.; te Riet, J.; Domanski, M.; Luttge, R.; Figdor, C. G.; Gardeniers, J. G.; Walboomers, X. F.; Jansen, J. A. Dynamic Cell Adhesion and Migration on Nanoscale Grooved Substrates. *Eur. Cells Mater.* **2012**, *23*, 182−193, discussion 193−194.
(34) Aonuma, H.; Ogura, N.; Takahashi, K.; Fujimoto, Y.; Iwai, S.; Hashimoto, H.; Ito, K.; Kamino, Y.; Kondoh, T. Characteristics and Osteogenic Differentiation of Stem/Progenitor Cells in the Human Dental Follicle Analyzed by Gene Expression Profiling. *Cell Tissue Res.* **2012**, *350*, 317−331.
(35) Rouahi, M.; Champion, E.; Hardouin, P.; Anselme, K. Quantitative Kinetic Analysis of Gene Expression During Human Osteoblastic Adhesion on Orthopaedic Materials. *Biomaterials* **2006**, *27*, 2829−2844.
(36) Wei, B.; Shang, Y. X.; Li, M.; Jiang, J.; Zhang, H. Cytoskeleton Changes of Airway Smooth Muscle Cells in Juvenile Rats with Airway Remodeling in Asthma and the RhoA/ROCK Signaling Pathway Mechanism. *GMR, Genet. Mol. Res.* **2014**, *13*, 559−569.
(37) Siebers, M. C.; ter Brugge, P. J.; Walboomers, X. F.; Jansen, J. A. Integrins as Linker Proteins Between Osteoblasts and Bone Replacing Materials. A Critical Review. *Biomaterials* **2005**, *26*, 137−146.
(38) Hamilton, D. W.; Brunette, D. M. The Effect of Substratum Topography on Osteoblast Adhesion Mediated Signal Transduction and Phosphorylation. *Biomaterials* **2007**, *28*, 1806−1819.
(39) Gandavarapu, N. R.; Mariner, P. D.; Schwartz, M. P.; Anseth, K. S. Extracellular matrix protein adsorption to phosphate-functionalized gels from serum promotes osteogenic differentiation of human mesenchymal stem cells. *Acta Biomater* **2013**, *9*, 4525−4534.
(40) Wang, G.; Zheng, L.; Zhao, H.; Miao, J.; Sun, C.; Liu, H.; Huang, Z.; Yu, X.; Wang, J.; Tao, X. Construction of a Fluorescent Nanostructured Chitosan-Hydroxyapatite Scaffold by Nanocrystallon Induced Biomimetic Mineralization and its Cell Biocompatibility. *ACS Appl. Mater. Interfaces* **2011**, *3*, 1692−1701.
(41) Tarone, G.; Hirsch, E.; Brancaccio, M.; De Acetis, M.; Barberis, L.; Balzac, F.; Retta, S. F.; Botta, C.; Altruda, F.; Silengo, L. Integrin

Function and Regulation in Development. *Int. J. Dev. Biol.* **2000**, *44*, 725−731.
(42) Aoudjit, F.; Vuori, K. Integrin Signaling in Cancer Cell Survival and Chemoresistance. *Chemother. Res. Pract.* **2012**, *2012*, 283181.
(43) Stuiver, I.; O'Toole, T. E. Regulation of integrin function and cellular adhesion. *Stem Cells.* **1995**, *13*, 250−262.
(44) Flick, M. J.; Du, X.; Degen, J. L. Fibrin(ogen)-Alpha M Beta 2 Interactions Regulate Leukocyte Function and Innate Immunity in Vivo. *Exp Biol. Med. (Maywood)* **2004**, *229*, 1105−1110.
(45) Rodan, S. B.; Rodan, G. A. Integrin Function in Osteoclasts. *J. Endocrinol* **1997**, *154* (Suppl), S47−56.
(46) Otawara-Hamamoto, Y. Biochemistry of bone matrix. *Nippon Rinsho* **1990**, *48*, 2729−2735.
(47) Mhanna, R. F.; Voros, J.; Zenobi-Wong, M. Layer-by-Layer Films made from Extracellular Matrix Macromolecules on Silicone Substrates. *Biomacromolecules* **2011**, *12*, 609−616.
(48) Heino, J. The Collagen Receptor Integrins have Distinct Ligand Recognition and Signaling Functions. *Matrix Biol.* **2000**, *19*, 319−323.
(49) Jiang, J.; Zhu, L.; Zhu, B.; Xu, Y. Surface Characteristics of a Self-Polymerized Dopamine Coating Deposited on Hydrophobic Polymer Films. *Langmuir* **2011**, *27*, 14180−14187.
(50) Leung, K. Cy5.5-Asp-Gly-Glu-Ala (DGEA). In *Molecular Imaging and Contrast Agent Database (MICAD)*; National Center for Biotechnology Information: Bethesda, MD, 2004.
(51) Linez-Bataillon, P.; Monchau, F.; Bigerelle, M.; Hildebrand, H. F. In Vitro MC3T3 Osteoblast Adhesion with Respect to Surface Roughness of Ti6Al4V Substrates. *Biomol. Eng.* **2002**, *19*, 133−141.
(52) Huang, H. H.; Ho, C. T.; Lee, T. H.; Lee, T. L.; Liao, K. K.; Chen, F. L. Effect of Surface Roughness of Ground Titanium on Initial Cell Adhesion. *Biomol. Eng.* **2004**, *21*, 93−97.
(53) Yang, Y.; Xia, T.; Zhi, W.; Wei, L.; Weng, J.; Zhang, C.; Li, X. Promotion of Skin Regeneration in Diabetic Rats by Electrospun Core-Sheath Fibers Loaded with Basic Fibroblast Growth Factor. *Biomaterials* **2011**, *32*, 4243−4254.
(54) Grayson, W. L.; Frohlich, M.; Yeager, K.; Bhumiratana, S.; Chan, M. E.; Cannizzaro, C.; Wan, L. Q.; Liu, X. S.; Guo, X. E.; Vunjak-Novakovic, G. Engineering Anatomically Shaped Human Bone Grafts. *Proc. Natl. Acad. Sci. U.S.A.* **2010**, *107*, 3299−3304.
(55) Liu, Q.; Cen, L.; Yin, S.; Chen, L.; Liu, G.; Chang, J.; Cui, L. A Comparative Study of Proliferation and Osteogenic Differentiation of Adipose-Derived Stem Cells on Akermanite and Beta-TCP Ceramics. *Biomaterials* **2008**, *29*, 4792−4799.
(56) Becker, D.; Geissler, U.; Hempel, U.; Bierbaum, S.; Scharnweber, D.; Worch, H.; Wenzel, K. W. Proliferation and Differentiation of Rat Calvarial Osteoblasts on Type I Collagen-Coated Titanium Alloy. *J. Biomed. Mater. Res.* **2002**, *59*, 516−527.
(57) Cowles, E. A.; Brailey, L. L.; Gronowicz, G. A. Integrin-Mediated Signaling Regulates AP-1 Transcription Factors and Proliferation in Osteoblasts. *J. Biomed. Mater. Res.* **2000**, *52*, 725−737.
(58) Carvalho, R. S.; Kostenuik, P. J.; Salih, E.; Bumann, A.; Gerstenfeld, L. C. Selective Adhesion of Osteoblastic Cells to Different Integrin Ligands Induces *Osteopontin Gene Expression*. *Matrix Biol.* **2003**, *22*, 241−249.
(59) La, W. G.; Shin, J. Y.; Bhang, S. H.; Jin, M.; Yoon, H. H.; Noh, S. S.; Im, G. I.; Kim, C. S.; Kim, B. S. Culture on a 3,4-Dihydroxy-L-Phenylalanine-Coated Surface Promotes the Osteogenic Differentiation of Human Mesenchymal Stem Cells. *Tissue Eng., Part A* **2013**, *19*, 1255−1263.